Transport of Ethylene Oxide Through Polymer Films

A. PHATAK,* C. M. BURNS, and R. Y. M. HUANG, *Department of Chemical Engineering, University of Waterloo, Waterloo, Ontario, Canada, N2L 3G1*

Synopsis

The transport of gaseous ethylene oxide (EtO) in several polymer films is studied using the carrier gas method of measurement. Permeability, solubility, and diffusion coefficients describing ethylene oxide (EtO) transport in polypropylene, polyvinylchloride, Teflon-FEP copolymer, and polyethylene films have been obtained over a 30 Celsius degree range at a low concentration of EtO using the carrier gas method of measurement. The results indicate that the diffusion of EtO in polyethylene is independent of penetrant concentration over the range of concentrations used. However, concentration-independent diffusion could not be verified directly for the other films studied. Two different techniques of determining diffusion coefficients were used, and within the precision of the data both yield the same result. An excess enthalpy of solution for the solubility of EtO in Teflon-FEP copolymer was calculated, an observation that suggests that dual-mode sorption may be taking place.

INTRODUCTION

In the medical products industry, ethylene oxide (EtO) is widely used as a gaseous sterilant.[1] However, since many of these products are frequently used well after sterilization, the need for packaging materials which maintain the sterility of the articles virtually indefinitely is quite apparent. Polymeric films such as those made of polyethylene and polyvinylchloride, or these plastics in combination with traditional packaging materials like kraft paper have proven quite successful in this regard.

Articles being treated invariably absorb some of the sterilant which has been shown recently to be a toxic substance.[2] Thus, while it is important that the sterility of the article be maintained, it is equally important that the ethylene oxide residues be allowed to dissipate from the sealed package. The package may, for example, be stored under ambient conditions for a considerable length of time or it may be degassed under vacuum. Hence, not only must the packaging film used act as a microbial barrier, it must also be sufficiently penetrable to EtO so that evacuation of the sterilant may take place within a reasonable period of time. How long a package must be stored before residual concentrations reach permissible levels will be determined by the solubility and diffusivity of the sterilant in the polymer.[3]

The present investigation is a continuation of work in our laboratory on the transport of gases through various polymer films.[4-8] The chief aim of the

*Present Address: Defence Research Establishment Valcartier, P.O. Box 8800, Courcelette, P.Q., Canada G0A 1R0.

Journal of Applied Polymer Science, Vol. 34, 1835–1859 (1987)
 CCC 0021-8995/87/051835-25$04.00

work reported in this paper is to characterize the transport of ethylene oxide in some typical polymeric films. To that end, we have constructed in our laboratory an apparatus based on the carrier gas method of measurement,[9-20] and have obtained permeability, solubility, and diffusion coefficients for several ethylene oxide/polymer pairs over a wide temperature range. Data such as these should be useful in recommending suitable packaging materials as well as in providing an overview of the nature of ethylene oxide transport in these polymers.

THEORETICAL PRINCIPLES

The diffusion of gases or vapors in polymer films can be adequately described by Fick's first law with a concentration-independent diffusion coefficient if there is no interaction between the polymer and diffusate.[21] Thus,

$$J/A = -D(dC/dx) \tag{1}$$

where J is the rate of transfer of permeant, A is the area of polymer through which diffusion takes place, D is the diffusion coefficient, C is the concentration of permeant in the polymer, and x is the space coordinate measured normal to the cross-sectional area of the polymer.[22] Indeed, even the diffusion of solvating vapors may be described by such a simple formalism in the limit of low activity of concentration of the vapor in the polymer.[23] In such an instance, the sorption of the diffusate at the surface of the polymer will follow Henry's law, which linearly relates the concentration of the penetrant at the surface of the film to its partial pressure, p, adjacent to polymer, i.e.,

$$C = Sp \tag{2}$$

where S is the Henry's law constant, or solubility coefficient. If the film is of thickness ℓ, and its faces at $x = 0$ and $x = \ell$ are maintained at concentrations $C = C_1$ and $C = C_2$, respectively, we can immediately integrate Eq. (1) to get an expression for the steady-state flow of diffusate through the polymer. Thus,

$$J_{ss} = D\frac{(C_1 - C_2)}{\ell} \tag{3}$$

where J_{ss} now refers to the steady-state flux, the rate of penetrant flow per unit area of polymer. It is clear from the above expression that the steady-state concentration gradient is a linear one.

Rearranging Eq. (3) to solve for D, the diffusion coefficient, yields

$$D = \frac{J_{ss}\ell}{(C_1 - C_2)} \tag{4}$$

Thus, if the quantities on the right-hand side of Eq. (4) are known or can be measured it is a simple matter to obtain the Fick's law diffusion coefficient. Frequently, however, it is impossible to measure surface concentrations directly; nevertheless, the partial pressure of permeant at the film surface is

usually known, and when Eq. (2) is substituted into Eq. (3), the resulting expression is

$$J = P\frac{(p_1 - p_2)}{\ell} \tag{5}$$

in which the product of the diffusion and solubility coefficients is replaced by P, the permeability coefficient. The term P describes the overall permeation process while S characterizes the sorption of permeant at the polymer surface and D, its passage through the matrix.

While Eq. (3) expresses steady-state flow, the transient diffusion of the permeant may be described by Fick's second law which, for a diffusion coefficient independent of penetrant concentration, is given by

$$\frac{\partial C}{\partial t} = D\frac{\partial^2 C}{\partial x^2} \tag{6}$$

The solution to Eq. (6) depends on the boundary conditions of the problem. In most studies of diffusion in polymers, it is quite common to expose a film, initially free of permeant, to a constant concentration or activity of gas at one face ($x = 0$) and then monitor the quantity of penetrant diffusing through the opposite surface, ensuring at the same time that the concentration at the downstream surface is negligible compared to the upstream concentration. Under such experimental constraints, the boundary conditions may be expressed mathematically as

$$C(x,0) = 0 \tag{7}$$

$$C(0,t) = C_1 \tag{8}$$

$$C(\ell,t) = 0 \tag{9}$$

The solution to Eq. (6) subject to the constraints defined above is

$$C(x,t) = -2\sum_{n=1}^{\infty}\frac{2C_1}{n\pi}\exp\left(\frac{-n^2\pi^2 Dt}{\ell^2}\right)\sin\frac{n\pi x}{\ell} - \left[C_1\frac{x}{\ell} - C_1\right] \tag{10}$$

and when this result is substituted into Eq. (1), we arrive at the following expression for the time-dependent penetrant flux:

$$J(t) = J_{ss}\left[1 + 2\sum_{n=1}^{\infty}(-1)^n\exp\left(\frac{-n^2\pi^2 Dt}{\ell^2}\right)\right] \tag{11}$$

If, for the polymer-penetrant system under investigation, the assumptions implicit in the derivation of Eq. (11) are valid, then Eq. (11) gives the response of the polymer film to a step change in penetrant concentration at one of its surfaces.

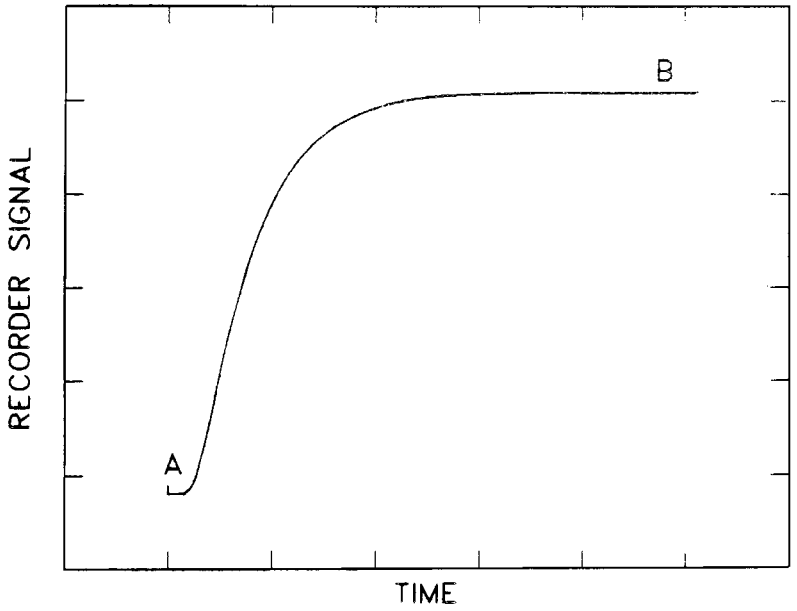

Fig. 1. Typical recorder trace.

CARRIER GAS METHOD OF MEASUREMENT

Numerous techniques for determining the transport parameters of gases and vapors in polymers exist, and they have been discussed in an extensive review by Lomax.[24,25] Of these experimental methods those that fall under the general heading of partition-cell methods have proven quite popular with workers in the field of transport in polymers. Although one particular partition-cell method, the high vacuum technique of Barrer,[26] has been the classical method of studying permeation through polymer films and membranes, in the last 20 years the carrier gas method or dynamic flow technique has been introduced as an alternative to it.

The carrier gas method was first conceived in the early 1900s[28] but was "reinvented" about 20 years ago.[9] In its simplest form, the carrier gas approach uses two streams of gas, both at nearly atmospheric pressure, flowing across each surface of a flat film or membrane which is clamped in a special permeability cell. Permeant gas or vapor is passed through the upstream chamber of the cell, while in the downstream compartment, flowing carrier gas picks up any permeant that has diffused through the polymer and transports it to a detector. The detector signal should be proportional to the permeation rate and hence to the penetrant flux [Eq. (11)]. It can be measured by an analog recorder or computer, for example, and the progress of the experiment can be conveniently monitored.

Figure 1 shows a typical recorder trace that might be obtained during the course of the permeation measurement. At point A, permeant is introduced into the system. The portion of the sigmoidal curve labelled AB represents the transient response of the system. At point B the steady-state concentration gradient has become fully developed and the flux remains invariant as long as the boundary conditions [Eqs. (8) and (9)] are maintained. Analysis of the

transient portion of the curve yields the diffusion coefficient while the permeability coefficient may be calculated knowing the steady-state flux of penetrant.

The carrier gas approach described above has the following advantages over the high vacuum technique of Barrer:

Since the permeability cell operates at or near atmospheric pressure on both sides of the film, little or no support for the polymer is required.

Operation at atmospheric pressure simulates conditions under which many plastic films are used. Packaging films are an example.

Simplicity of design and operation at atmospheric pressure largely eliminate the problem of leaks in the system.

MATHEMATICAL TREATMENT OF EXPERIMENTAL RESULTS

The calculation of permeability coefficients from the recorder trace shown in Figure 1 is quite straightforward. Once the detector has been calibrated with known concentrations of penetrant, the steady-state signal can be converted to the steady-state permeation rate. Then, knowing the film thickness and the difference in penetrant partial pressure across the film, P may be calculated by rearranging Eq. (5). There are, however, several means by which the transient part of the permeation curve may be analyzed to elicit the diffusion coefficient.[10,11,13,15,28] We have used only two of them.

The simpler of the two methods is known as the half-time method, and it was first outlined by Ziegel, Frensdorff, and Blair.[10] If $t_{1/2}$ denotes the time required for the penetrant flux to reach half its steady-state value, then $J/J_{ss} = 1/2$ at $t = t_{1/2}$. Substituting this into Eq. (8) and solving for D, we obtain

$$D = \frac{\ell^2}{7.2t_{1/2}} \tag{12}$$

In most carrier gas systems there is a finite amount of time required for the penetrant gas or vapor to reach the surface of the film from its source. As well, the carrier gas-penetrant mixture also requires a certain amount of time to flow from the downstream side of the permeability cell to the detector. Thus, the half-time obtained from the recorder trace, $t'_{1/2}$, must be corrected for these time lags. An estimate of the "true" half-time, $t_{1/2}$, may be obtained by subtracting from $t'_{1/2}$ all time lags. Such a procedure amounts to shifting the recorder trace or permeation curve along the abscissa. The sum of the lags may be determined by measuring the time required for a signal to be recorded when a step change in concentration is introduced on one side of a metallic film containing a pinhole.[28] Alternatively, the lags may be estimated by summing up the residence time of the gas or vapor in the various system components.

In the second method, known as the method of moments,[15,29,30] the time-varying signal of the detector is not considered as a measure of the response of the polymer film to a step change in concentration. Instead, it considers the resulting signal a measure of the response of the entire system to the unit step

input. The contribution of the other components (the cell, the detector, and the connecting tubing) can be factored out, thereby isolating the response of the film alone. From this response, the diffusion coefficient may be calculated by an equation similar in form to Eq. (9). The characteristic time in this method, denoted M_o, is calculated by integrating the quantity $1 - J/J_{ss}$ from $t = 0$ to $t = \infty$. Because of the time lags inherent in the system, however, $J(t)$ is not equivalent to $R(t)$, the instantaneous detector signal. Hence, a quantity analogous to M_o which represents the characteristic time of the entire system must first be calculated. This quantity, M_o', is given by

$$M_o' = \int_0^\infty (1 - R(t)/R_{ss})\, dt \tag{13}$$

where R_{ss} is the asymptotic value of the recorder signal. The contribution of all the system components except the polymer may then be factored out by simply subtracting the value of their time lags from M_o', thereby leaving only the pure lag due to polymer. Thus

$$M_o = M_o' - \Sigma\tau_i \tag{14}$$

where $\Sigma\tau_i$ represents the sum of the lags due to the connecting tubing, the compartments of the permeability cell, and the lag inherent in the detector itself. Felder et al.[29] provide a theoretical basis for the deconvolution and show that lags due to tubing and compartments are simply the residence times of the permeant gas or vapor in those components. The detector lag is usually small compared to the other delays in the system although it can also be estimated.[29] Moreover, it has also been shown that M_o is equivalent to the time lag, θ, of the Barrer high vacuum method. Thus, the expression for the diffusion coefficient is simply

$$D = \frac{\ell^2}{6M_o} \tag{15}$$

Once P and D have been calculated, the Henry's law solubility coefficient, S, may be determined by calculating the ratio of the permeability and diffusion coefficients.

EXPERIMENTAL DETAILS

Materials

All gases and gas mixtures were obtained from the Linde Division of Union Carbide Limited. The carrier gas was helium with a purity greater than 99.996% and an oxygen content not exceeding 3 ppm. For calibration of the detector and for experimental runs, mixtures of ethylene oxide in helium were used. Mixtures with an EtO concentration greater than 50 ppm were made to a tolerance of $\pm 5\%$ while those containing less than 50 ppm were made to $\pm 3\%$.

The polymer films used in this study were obtained from three different sources. Polyethylene films of three different densities [linear low (LLDPE), medium (MDPE), and high (HDPE)] were obtained from DuPont Canada (Kingston, Ontario) as was the polyvinylchloride film (PVC), although its origin is uncertain. The Teflon-FEP (TEF-FEP) copolymer film was taken from existing stocks in this laboratory and had been originally supplied by the

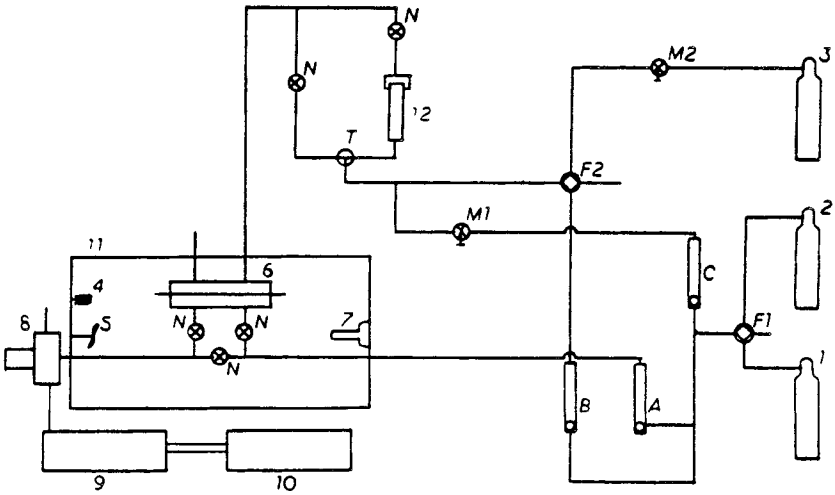

Fig. 2. Permeation apparatus: (A, B, C) high precision rollers; (F1, F2) four-way valves; (M1, M2) metering valves; (N) needles; (1) Helium supply; (2) calibration mixture; (3) permeant gas; (4) 150W light bulb; (5) circulating fan; (6) permeability cell; (7) temperature controller; (8) photoionization detector; (9) electrometer/power supply; (10) stripchart recorder; (11) insulated box; (12) mixing tube.

Plastics Department, Fluorocarbon Division of E. I. DuPont de Nemours and Company, Inc. (Circleville, Ohio). Polypropylene (PP) sheet was supplied by the film division of Mobil Chemical Canada, Ltd. (Belleville, Ontario). All films were nominally 0.0025 cm thick with the exception of the PVC film which was 0.002 cm thick and the high-density polyethylene film which was 0.0019 cm thick.

Apparatus

The carrier gas apparatus in our laboratory, shown schematically in Figure 2, is based on designs described in the literature.[9,11,28] The permeability cell consists of two pieces of type 304 stainless steel, each having a 2-inch diameter, circular recess machined into its surface. When a test film is inserted into the cell, two compartments are formed. Each compartment has a volume of approximately 1 cm^3. Surrounding the lower cavity is an O-ring of Buna-N rubber, which seals the cavities and prevents leaks into or out of the cell. The area of the film exposed to permeant is not defined by the O-ring, however, but by the edges of the cavities. When the cell is clamped shut a metal-film-metal seal is formed. Four corner-bolts pass through both halves of the cell, and uniform compression is provided by tightening wing nuts at each corner. In each cavity inlets and outlets for gas flow are placed as far apart as possible so efficient sweeping of both surfaces of the film can take place.

The entire cell and a portion of the lines leading to and from it were enclosed by a thermostatted oven. The oven consists of a double-walled, insulated box constructed of heavy gauge aluminum sheet. Internal temperature was regulated by a temperature regulator connected to a low wattage heater, which in this case was a 150 W light bulb. A small fan provided the necessary air circulation. This simple design gave remarkably good tempera-

ture control (±1°C) up to 60°C. During the experiments the temperature inside the oven was monitored by a copper-constantan thermocouple.

All gas lines were made of 1/8 in. OD stainless steel tubing. Flows were monitored by Matheson Ltd. and Broods Ltd. precision flowmeters fitted with high accuracy valves. Fittings connecting the tubing to the various components were commercially available compression type. The mixing tube shown in Figure 2 (item 12) consists of a four-inch length of 1 in. OD type 316 stainless steel pipe packed throughout with 3 mm glass beads. Its void volume, measured by filling the tube with water, was approximately 23 cm^3. When ethylene oxide standards were diluted with pure carrier gas the resulting mixtures were sent through the mixing tube to ensure thorough comingling.

The outflow from the lower compartment of the cell is connected directly to a photoionization detector (PID) (HNU Systems Inc., PI 52-02). In the photoionization detector, ionization takes place in a disc-shaped chamber, one face of which is the window of a sealed lamp which emits monochromatic radiation in the ultraviolet (UV) range. A molecular species having an ionization potential less than the energy of the UV lamp will be ionized upon passing through the chamber. The ions resulting from this photoionization are driven to a collector electrode by applying a positively biased high voltage, and the current produced is directly proportional to the concentration of that species.[31] In practice, the PID will detect molecules with an ionization potential (IP) up to 0.3 eV greater than the lamp energy. Thus, to detect EtO (IP = 10.565 eV) lamps with energies of 10.2 eV and 11.7 eV were used.

The PID was coupled to an HNU electrometer/power supply (EPS) which supplied the necessary high voltage for firing the UV lamp and accelerating the ions to the collector electrode. The EPS also contained a rheostat for adjusting the power to the detector and a pyrometer for reading the detector temperature. Lamp intensity could be adjusted from the EPS unit. As intensity was increased, sensitivity increased as well, although only at the cost of greater baseline instability. During the course of a run the detector signal was recorded continuously on a Watanabe CH1 recorder set at 10 mV full scale deflection.

Procedure

Detector Calibration

The photoionization detector was calibrated with standards of EtO in helium which ranged in concentration from 1 to 1000 ppm. It showed a linear response with ethylene oxide concentrations between 3 and 1000 ppm. Below 3 ppm the detector response was only slightly nonlinear, while well above 1000 ppm, severe quenching of the detector signal occurred. Figure 3 shows the response of the PID with the 10.2 eV lamp up to 100 ppm.

Transport Measurements

Films were cut into strips of roughly 8 cm by 12 cm and then carefully examined for macroscopic defects. If the sample was creased, pitted, or contained any other readily visible flaws it was discarded. Prior to an experimental run the test strip was first rinsed with deionized water and then

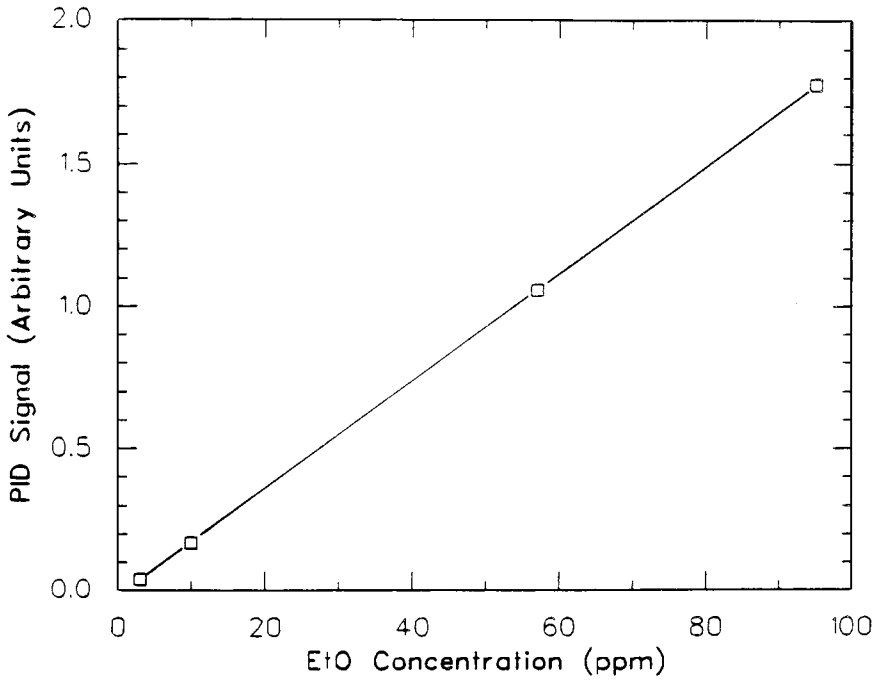

Fig. 3. Calibration curve for PID with 10.2 eV lamp.

vacuum-dried at room temperature for, on average, two hours. It was then placed in the cell and flushed with helium for another four to six hours.

Once the detector and cell temperature had stabilized, the flow of penetrant to the polymer could be initiated by switching the four-way valve labelled F2 in Figure 2. The flow from the penetrant tank was regulated by the metering valve M2, and could be set before the run by attaching a soap bubble flowmeter to the exhaust port of the four-way valve. The carrier gas flow rate was also monitored with a soap bubble flowmeter before an experiment and intermittently during it.

The permeant used was a mixture of ethylene oxide in helium. Pure helium swept the downstream surface of the film. Steady-state flow of ethylene oxide was presumed when the recorder signal remained invariant for three to five minutes.

Calculations

Permeability, diffusion, and solubility coefficients were calculated by the methods outlined earlier. The value of M_o' was calculated by first determining the value of the integral $\int_0^\infty (R_{ss} - R(t))\, dt$ and then dividing by R_{ss}. Integration was carried out graphically by using a Keuffel and Esser Model 62-0005 Compensating Plane Polar Planimeter.

RESULTS AND DISCUSSION

In one of the few published studies of EtO transport in polymeric films, Waack et al.[32] found that permeability coefficients were dependent on per-

meant concentration. The range of EtO partial pressures to which the films were exposed extended from 8 cm Hg to 35 cm Hg. The passage of organic vapors and liquids through polymeric materials is frequently characterized by such concentration-dependent transport. Nevertheless, it has been shown that in the limit of low penetrant activity, even the diffusion of solvating vapors can be described by concentration-independent Fickian diffusion.[23] Many authors have made use of this mathematically and experimentally advantageous situation when making transport measurements.[28,30,32] Thus, in this study, the maximum partial pressure of EtO to which any of the films was exposed was about 0.76 cm Hg. The permeant gas consisted of a mixture of roughly 1% ethylene oxide in helium.

Effect of Concentration

A single permeation rate experiment, unlike its sorption counterpart, cannot verify the assumption of concentration-independent diffusion directly. It is necessary to measure and compare transport parameters over a range of permeant concentrations or partial pressures.

According to the method of Duncan et al.[30] if a plot of steady-state penetrant flux versus p/ℓ for a particular film is linear, then the ideal solution-diffusion model can be assumed, and the slope of the line will be the permeability coefficient P. The mathematical formulation is

$$J_{ss} = P\frac{p}{\ell} \tag{16}$$

in which the partial pressure difference across the film is given by the partial pressure of the EtO in the permeant gas because the concentration at the downstream surface of the film is zero. Figure 4 shows that such a relationship holds for the permeation of EtO through 0.0019-cm thick high-density polyethylene at 30°C. The slope of the least-squares fitted line, P, is 18.5×10^{-10} cm^3 (STP) cm/s cm^2 cm Hg. The concentrations at the extremities of the abscissa represent commercially prepared mixtures of 1080 ppm and 10,200 ppm while intermediate values represent mixtures made by diluting a stream of 1.02% EtO in helium with pure carrier gas to achieve the approximate desired concentrations. Hence, for this high-density polyethylene film, diffusion can be described by concentration-independent Fickian diffusion between approximately 0.07 cm Hg and 0.7 cm Hg. It is likely that this behavior extends to the other polyethylene films.

None of the other films could be tested in a like manner because of their low permeabilities. Thus, although it can be presumed that transport through PVC, PP, and Teflon-FEP copolymer films is concentration independent because of the low penetrant concentration encountered, the results for these films should be used with caution, keeping in mind the conditions under which the measurements have been made.

Permeability Coefficients

Permeability coefficients were measured for the six films over a 30 Celsius degree temperature range. The linearity of the Arrhenius plots in Figures 5 and 6 indicate that within the temperature range shown (approximately

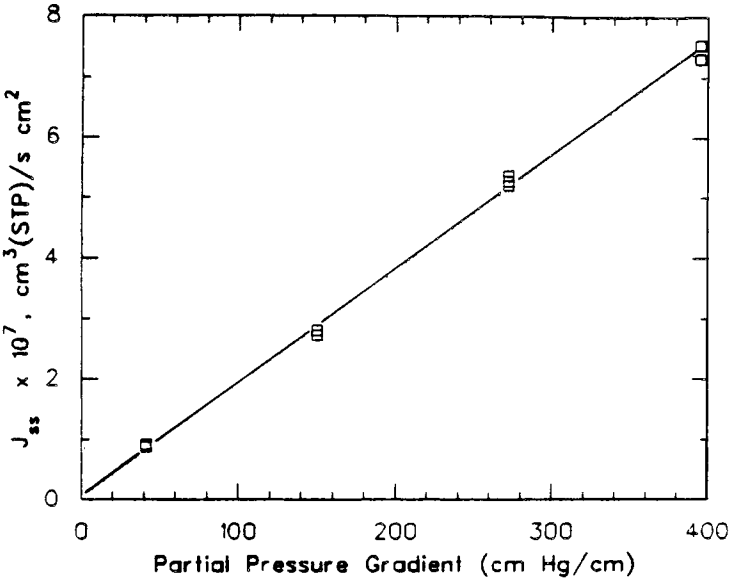

Fig. 4. Effect of EtO partial pressure on steady state flux. (0.0019 cm HDPE.)

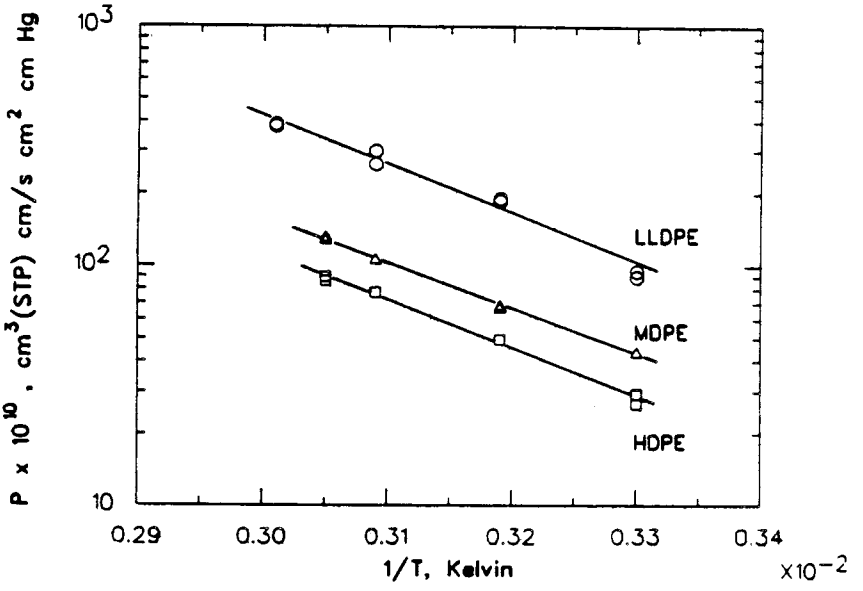

Fig. 5. Arrhenius plot of EtO permeability coefficients. (Polyethylene Films.)

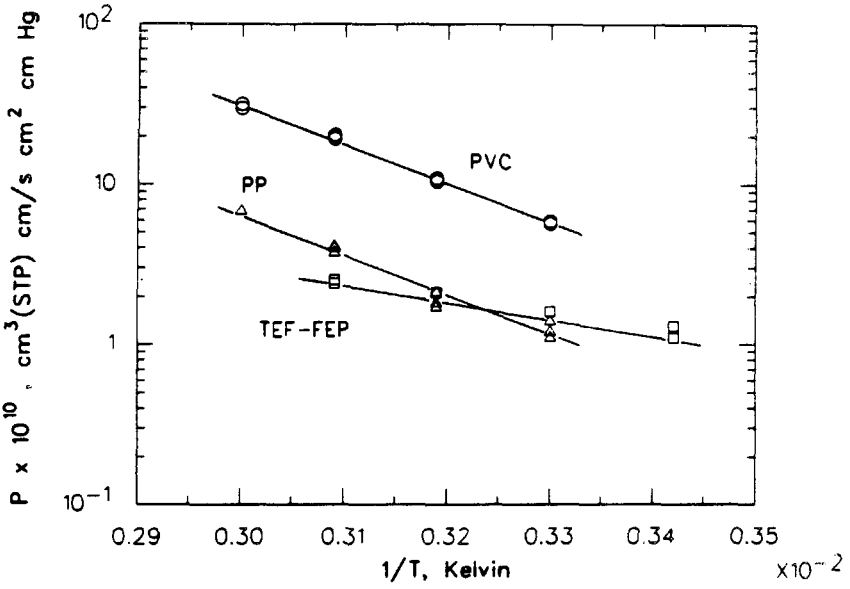

Fig. 6. Arrhenius plot of EtO permeability coefficients. (PVC, PP, and TEF-FEP.)

20°C–60°C), the process of permeation can be satisfactorily described by the expression

$$P = P_o \exp(-E_p/RT) \tag{17}$$

P_o, the pre-exponential factor, and E_p, the activation energy for permeation, are listed in Table I along with permeability coefficients at 30°C.

Waack et al.[32] determined the permeability coefficient of EtO in several films at various partial pressures. At a partial pressure of 8.1 cm Hg, the lowest value at which transport measurements were made, the permeability of EtO through low-density polyethylene film we reported to be 22×10^{-10} cm^3

TABLE I
Permeability Data for Ethylene Oxide

Films	$P \times 10^{10}$ (30°C) $\frac{\text{cm}^3\text{ (STP) cm}}{\text{s cm}^2\text{ cm Hg}}$	P_o	E_P cal/mol	% Crystallinity[a]
LLDPE	91.8(20)[b]	.135	9890	31.2
MDPE	43.1(20)	.007	8650	38.8
HDPE	28.5(20)	.011	9130	46.6
PVC	5.8(10)	.073	11150	—
PP	1.2(20)	.039	11750	—
TEF-FEP	1.1(15)	6.7×10^{-7}	4970	—

[a] From differential scanning calorimetry (DSC) measurements.
[b] Figures in parentheses are uncertainties expressed as a percentage.

(STP) cm/s cm^2 cm Hg at 0°C. If the Arrhenius plot for LLDPE (Fig. 5) is extended to 0°C, the apparent permeability coefficient at that temperature is 16×10^{-10} cm^3 (STP) cm/s cm^2 cm Hg.

As a group, the polyethylene films are more permeable to ethylene oxide than the other films studied. In semicrystalline polymers like polyethylene, sorption and diffusion are believed to occur exclusively in the amorphous regions of the polymer.[25] As amorphous content increases permeability should also increase. The data in Table I show that the permeability of the polyethylene films increases as the crystallinity decreases from 46% to 31%. Figure 5 and the data in Table I also show that the activation energy for permeation is roughly the same for low, medium, and high-density polyethylene films. If, indeed, transport does take place solely through amorphous regions then such a similarity would not be unexpected since the amorphous environment is likely quite similar in all three samples.

In some instances the point at which steady-state flow through the polymer was reached was difficult to identify unambiguously on the recorder trace. This difficulty was due primarily to the fluctuation of temperature within the oven surrounding the cell and a slight temperature drift of the detector block. It is partly reflected in the estimates of uncertainty shown in Table I. A more complete discussion of the uncertainties in all the coefficients calculated may be found elsewhere.[35] Precise identification of steady state is important not only in the determination of P, but also in the determination of the diffusion coefficient.

Diffusion Coefficients

For all films except polypropylene, diffusion coefficients were calculated by the two methods outlined above. Diffusion coefficients calculated by the half-time method are denoted D_H while those determined by the method of moments are denoted D_M. Their variation with temperature is shown in Figures 7 to 11. The activation energy for diffusion, E_d, and the pre-exponential factor D_o, derived by fitting an Arrhenius expression to the data, are summarized in Table II. The linearity of the plots confirms that little or no interaction takes place between polymer and penetrant.

The activation energy, E_d, is a fundamental parameter associated with the energy required for hole formation, that is, the energy required to separate the polymer chain segments so that passage of a penetrant molecule can occur. If we consider the glass transition (T_g) temperature of a polymer to be a qualitative measure of chain stiffness, we would then expect that a higher T_g (and hence, greater chain stiffness) results in a higher E_d. Correlating the activation energies shown in Table II with the T_gs of the respective polymers we see that the E_d for diffusion through polyethylene films ($T_g \approx -120$°C) is lower than the E_d for diffusion through PP, PVC, and Teflon-FEP, polymers which have much higher glass transition temperatures. Furthermore, a comparison of diffusion coefficients at 30°C with glass-transition temperatures indicates that as T_g (and hence, chain stiffness) increases, the diffusion coefficient decreases.

The activation energies listed in Table II range from 7 kcal/mol to 15 kcal/mol. Some authors[38,39] have pointed out that anomalous diffusion such

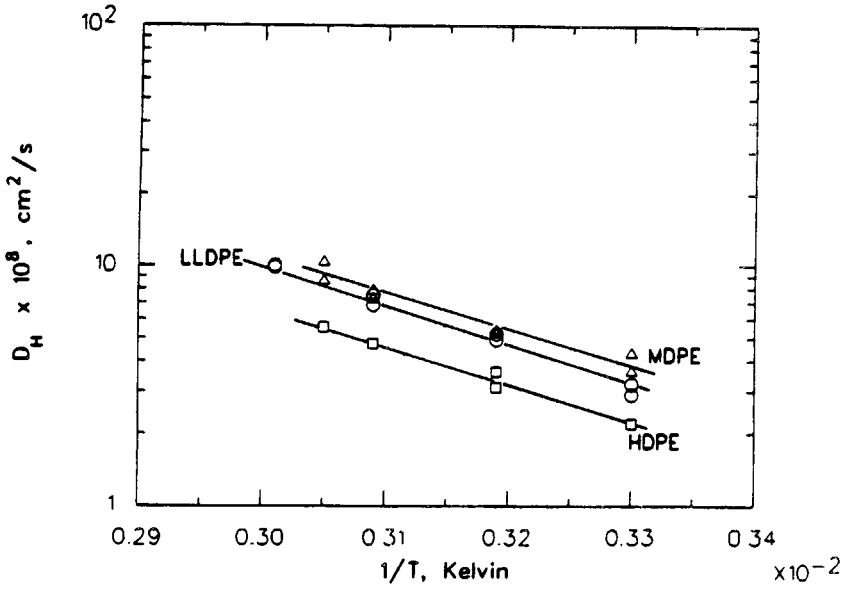

Fig. 7. Arrhenius plot of EtO diffusion coefficients. (D_H, Polyethylene films.)

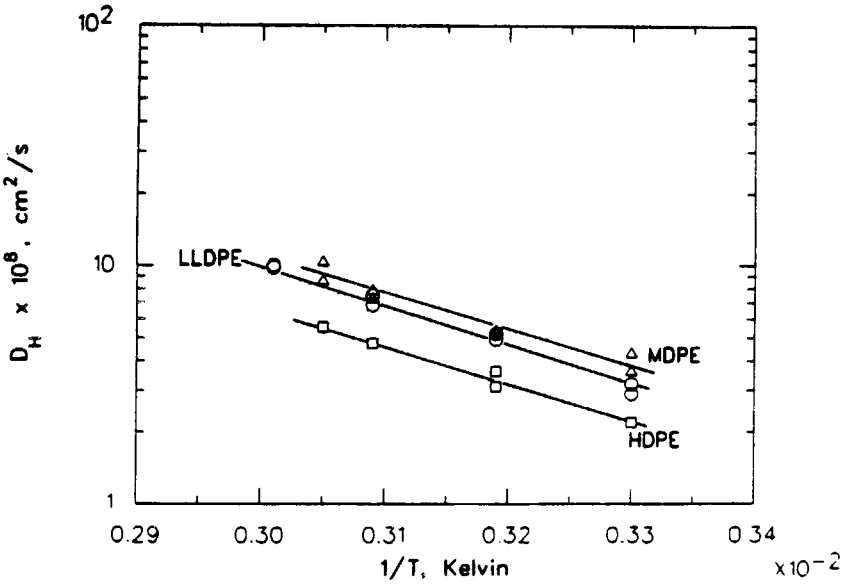

Fig. 8. Arrhenius plot of EtO diffusion coefficients. (D_M, Polyethylene films.)

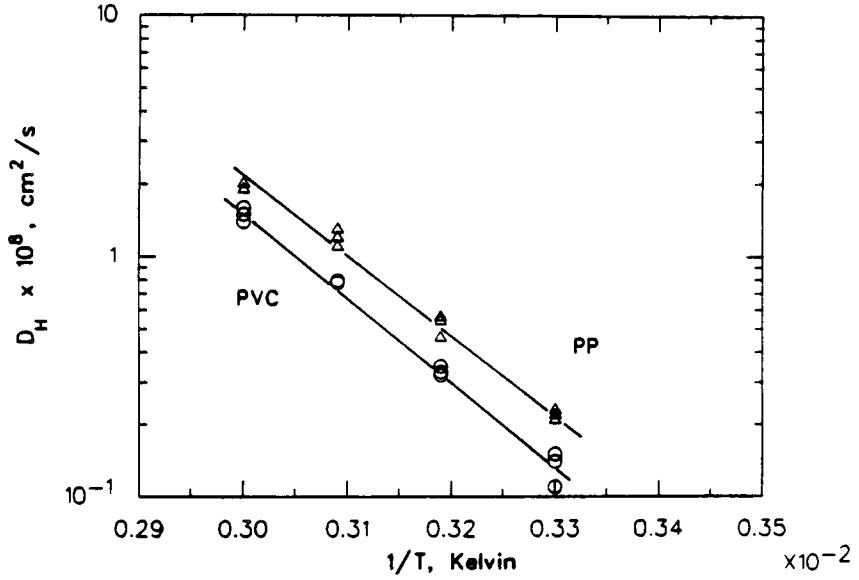

Fig. 9. Arrhenius plot of EtO diffusion coefficients. (D_H, PP and PVC.)

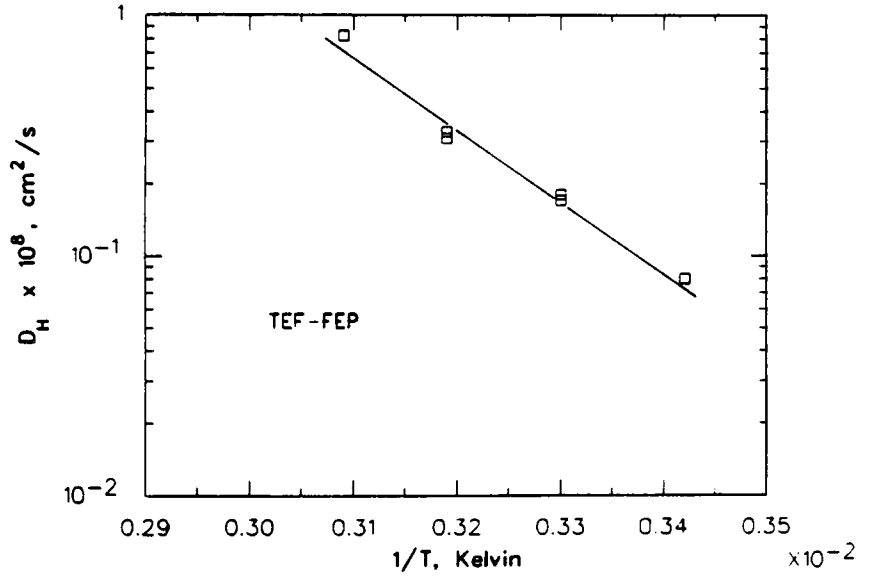

Fig. 10. Arrhenius plot of EtO diffusion coefficients. (D_H, TEF-FEP.)

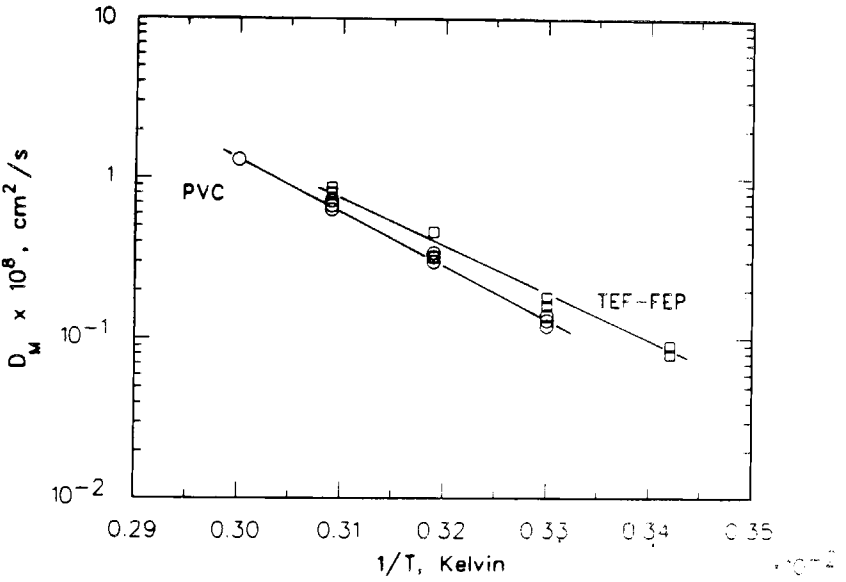

Fig. 11. Arrhenius plot of EtO diffusion coefficients. (D_M, PVC and TEF-FEP.)

TABLE II
Diffusivity Data for Ethylene Oxide

	$D_H \times 10^8$ cm^2/s (30°C)		Half-time		Method of moments		
				E_d		E_d	T_g
Films	D_H	D_M	D_o	cal/mol	D_o	cal/mol	°C
LLDPE	3.1(25)[a]	3.2(25)	.0172	7950	.012	7760	
MDPE	3.8(25)	3.6(25)	.0044	7025	.0004	5700	−120[c]
HDPE	2.1(15)	2.3(15)	.0054	7475	.0007	6220	
PVC	.13(15)	.13(10)	642	16180	156	15350	39[b]
PP	.22(20)	—	[illegible]	15000	—	—	−6[b]
TEF-FEP	.17(15)	.17(15)	47	14470	47	14450	126[d]

[a] Figures in parentheses are uncertainties expressed as a percentage.
[b] From DSC measurements; PVC contains unknown amount of plasticizer.
[c] From Ref. 36.
[d] From Ref. 37, T_g of polytetrafluoroethylene.

as Case II diffusion is usually associated with much higher activation energies than Fickian diffusion. Although no range of values appropriate to Fickian diffusion can be distinctly defined, a comparison of the energies in Table II with the data of Stannett[21] reveals that a range of 7–15 kcal/mol corresponds to the activation energy for the diffusion of simple gases in high polymers, a phenomenon which follows the Fickian model.

The E_d values for the polyethylene films are, like the E_p values, nearly equal. There is no observable trend among them, and given the error associ-

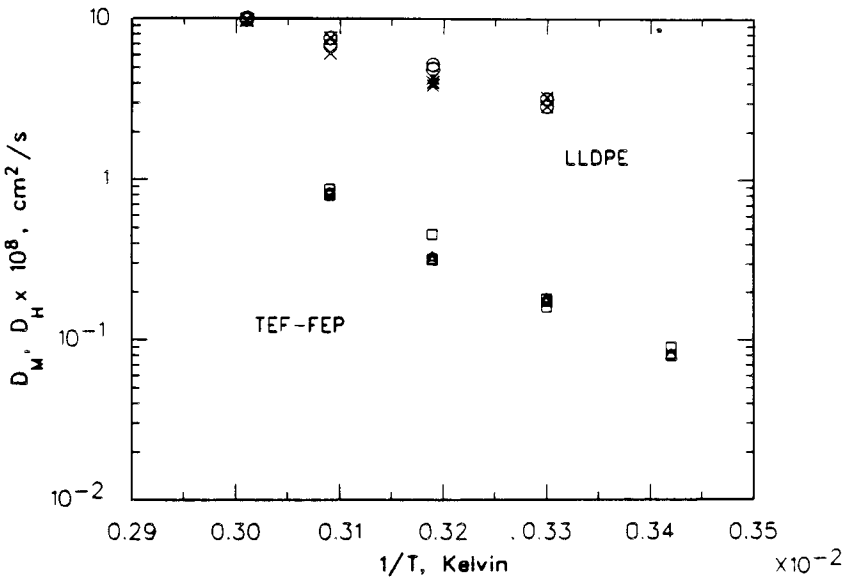

Fig. 12. Comparison of D_H and D_M. (LLDPE and TEF-FEP): (○, △) D_H; (×, □) D_M.

ated with them, it is likely that they are not significantly different from one another. Again, if the environment through which the penetrant diffuses is similar in the three polyethylene films, the activation energies would also be nearly equivalent.

In general, half-time diffusion coefficients agreed well with diffusion coefficients calculated by the method of moments. Values of D_H and D_M at 30°C are shown in Table II for all films except polypropylene, and in Figures 12 to 14 D_M and D_H are shown on the same graph for LLDPE, MDPE, PVC, and TEF-FEP. It can be seen that, within the precision of the data, diffusion coefficients determined by the half-time method and method of moments are not significantly different. Neither method of determining diffusion coefficients, however, deals adequately with the difficulties that arise when the characteristic times, M_o or $t_{1/2}$, are on the same order of magnitude as the equipment lags. For relatively permeable films such as polyethylene at higher temperatures, the characteristic time, M_o or $t_{1/2}$, is of the same order of magnitude as the lags inherent in the permeation equipment. Thus the determination of the diffusion coefficient becomes extremely sensitive to the uncertainty in the value of the time delay. However, for smaller diffusion coefficients, that is, larger characteristic times, the time delay can be ignored. For example, the apparent half-time for the diffusion of EtO in Teflon-FEP at 20°C is about 1000 s. Disregarding the delay of approximately 20 s results in an error of only 2% in the calculated result.

Such observations point to a deficiency in the carrier gas technique. Namely, because of the sensitivity of the diffusion coefficient to the equipment lag with very fast films, the dynamic flow method may be more suited to less perme-

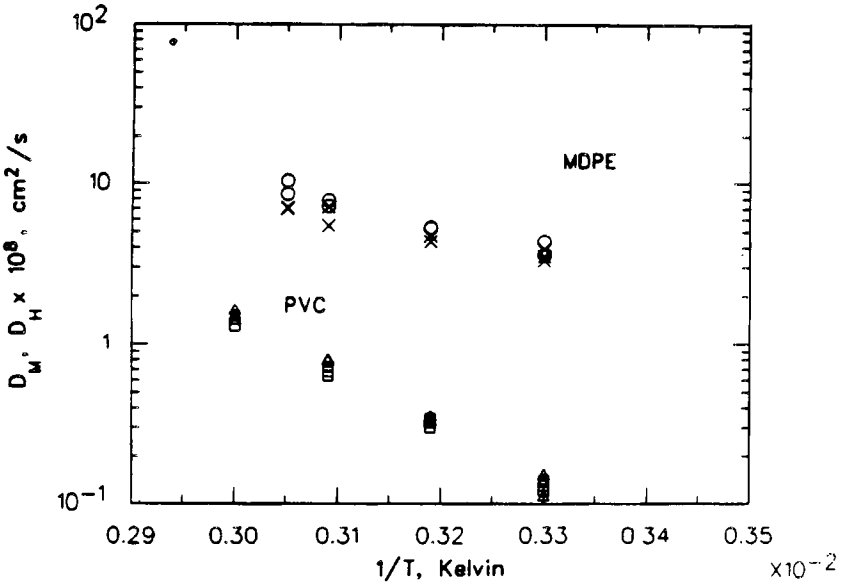

Fig. 13. Comparison of D_H and D_M. (MDPE and PVC): (○, △) D_H; (×, □) D_M.

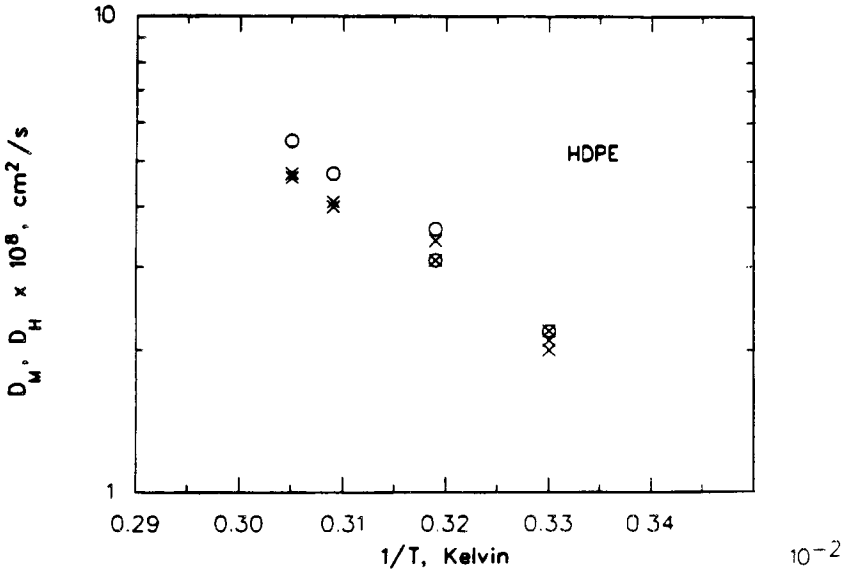

Fig. 14. Comparison of D_H and D_M. (HDPE): (○) D_H; (×) D_M.

TABLE III
Solubility Data for Ethylene Oxide

Films	S (30°C) cm^3 (STP) / cm^3 cm Hg S_H	S_M	Half-time S_o	Half-time ΔH_s (cal/mol)	Moments S_o	Moments ΔH_s (cal/mol)	δ $(cal/cm^3)^{1/2}$
LLDPE	.01[a]	.29(40)	7.8	1940	11.3	2130	
MDPE	.(35)	.11(28)	1.7	1620	16.4	2940	7.8[b]
HDPE	.13(25)	.14(25)	2.1	1660	16.8	2910	
PVC	.44(20)	.45(15)	.0001	−5030	.0004	−4200	9.4–10.8[b]
PP	.06(28)	—	.0003	−3250	—	—	8.3[c]
TEF-FEP	.09(20)	.12(20)	2.3×10^{-8}	−9190	1.8×10^{-8}	−9160	—

[a] Figures in parentheses are uncertainties expressed as a percentage.
[b] Ref. 37.
[c] Ref. 36.

able films. At the other extreme, however, detector instability at very high sensitivities over a long period of time makes the method less suitable for highly impermeable films. Other authors[13] have recommended that the carrier gas method be used with moderately permeable films only. Nevertheless, despite misgivings that it is based on a single point, the half-time method is a remarkably robust method which provides estimates of the diffusion coefficient quickly and easily.

Solubility Coefficients

Solubility coefficients were determined by calculating the quotient P/D. Shown in Table III are solubility coefficients at 30°C, along with the parameters obtained by fitting the data to the van't Hoff expression

$$S = S_o \exp(-\Delta H_s/RT) \tag{18}$$

ΔH_s is the heat of solution of penetrant in the polymer and S_o is the pre-exponential factor. Because S is obtained indirectly in most partition-cell methods like the carrier gas technique, the uncertainties in the permeability and diffusion coefficients are both reflected in the error associated with the solubility coefficients. Uncertainties for the six films studied are also listed in Table III. In some instances the resultant errors can be large enough to obscure the effect of temperature on solubility. For example, the correlation between $\log S$ and $1/T$ for polypropylene (Fig. 15) is a poor one. However, given that P and D follow Arrhenius dependencies for PP, and indeed for all other films, scatter in the van't Hoff plots (Figs. 15–19) is probably not due to any sorption anomalies. The heat of solution ΔH_s, obtained from S_H differs markedly with that obtained from S_M, but by examining the relative magnitudes of ΔH_s and S for all films rather than their absolute magnitudes it is still possible to draw some meaningful conclusions.

Chemical similarity between the polymer and sorbate is a major factor determining the extent of solubility. The square root of the cohesive energy density, or δ, its solubility parameter, is frequently used to predict solubility

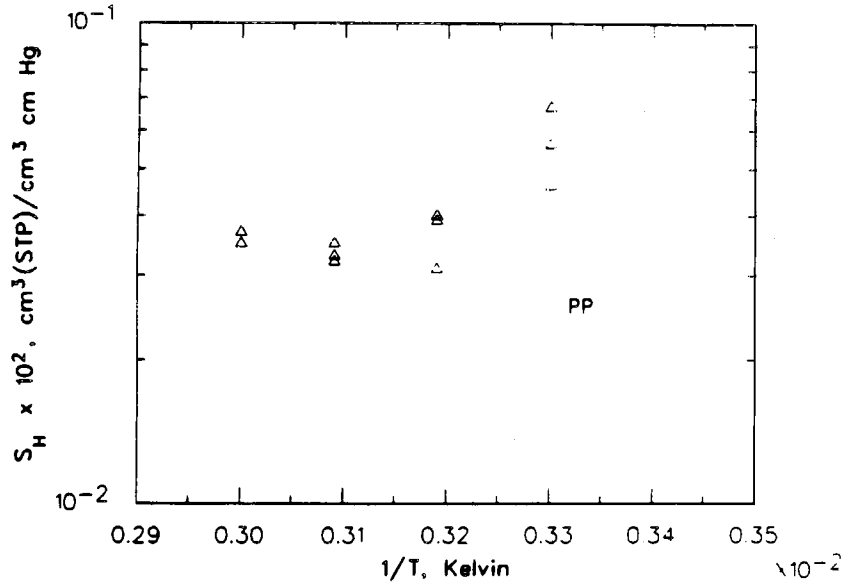

Fig. 15. Van't Hoff plot of EtO solubility coefficients. (S_H, PP.)

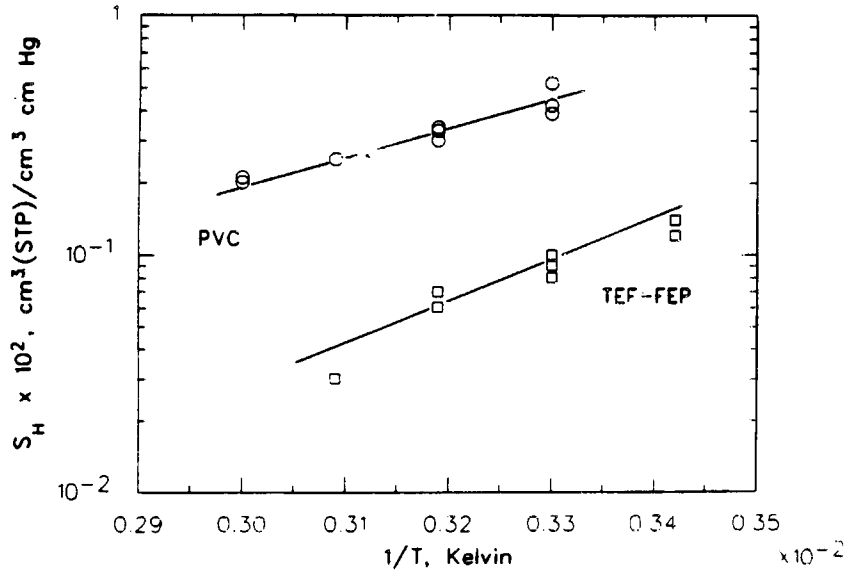

Fig. 16. Van't Hoff plot of HtO solubility coefficients. (S_H, PVC and TEF-FEP.)

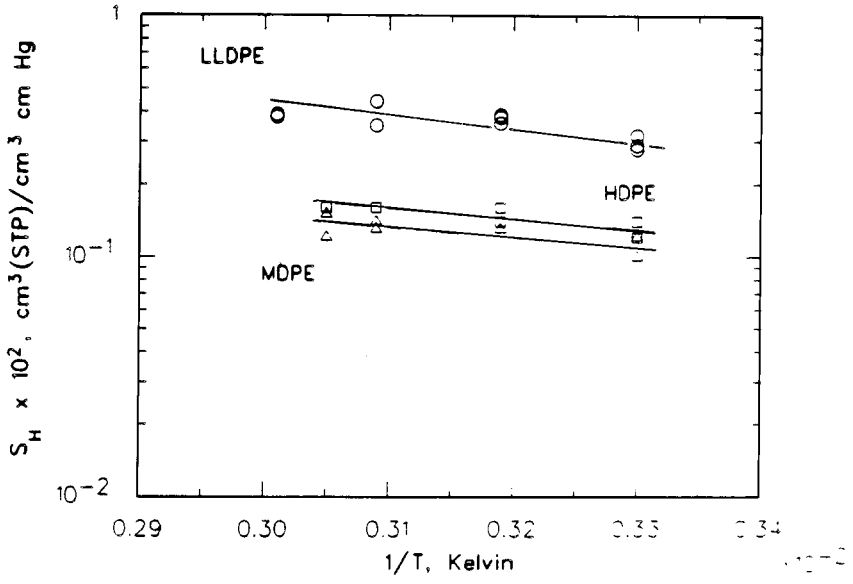

Fig. 17. Van't Hoff plot of EtO solubility coefficients. (S_H, Polyethylene films.)

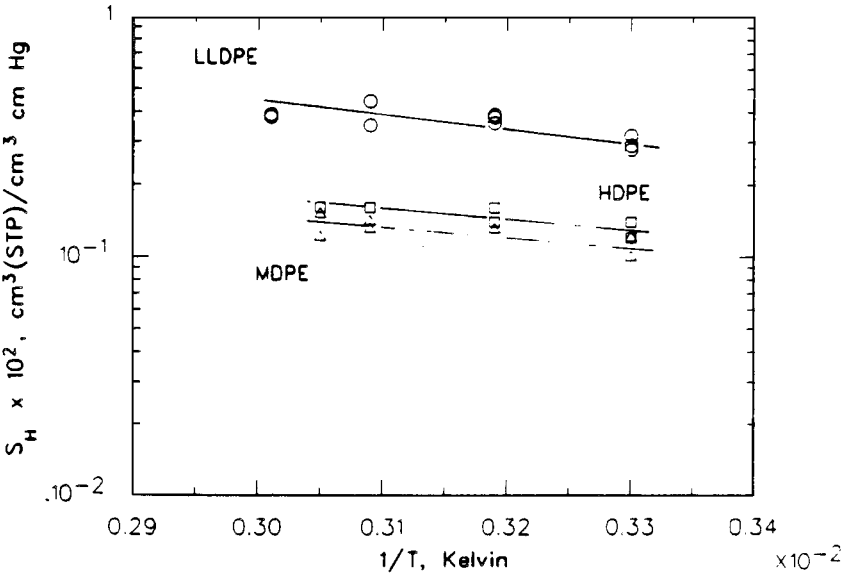

Fig. 18. Van't Hoff plot of EtO solubility coefficients. (S_M, Polyethylene films.)

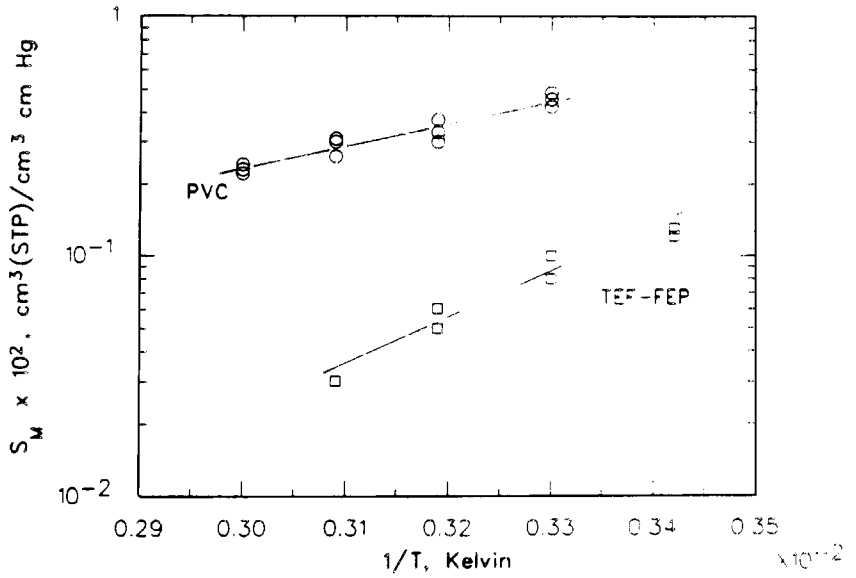

Fig. 19. Van't Hoff plot of EtO solubility coefficients. (S_M, PVC and TEF-FEP.)

and compatibility. As the δ values of a polymer and penetrant become more equal, the solubility of that sorbate should increase. The δ value of EtO is 11.1 $(cal/cm^3)^{1/2}$,[40] and comparing its solubility in PVC and polyethylene in Table III we see that EtO is more soluble in PVC, a polymer whose solubility parameter is numerically closer to 11.1 $(cal/cm^3)^{1/2}$.

The sorption of a penetrant onto the surface of a polymer can be considered as a two-stage process: first, condensation of the vapor followed by mixing of the condensed vapor with the polymer.[41] Associated with the first step is the molar heat of condensation of the permeant, ΔH_c, and with the second step, the partial molar heat of mixing, ΔH_m. Thus,

$$\Delta H_s = \Delta H_m + \Delta H_c \tag{19}$$

The value of ΔH_m can be estimated by means of the Hildebrand equation, i.e.,

$$\Delta H_m = \bar{V}_1(\delta_1 - \delta_2)^2\phi_2^2 \tag{20}$$

The volume fraction of polymer, usually unity in the case of a dilute solution, is denoted by ϕ_2, and $\bar{V}_1$ represents the partial molar volume of the penetrant in the polymer.

For gases well above their critical points, the hypothetical ... of ΔH_c is negligible and therefore ΔH_s is determined by ΔH_m which is positive and usually quite small.[42] Thus, the solubility coefficient increases with temperature. For more condensible vapors and gases the heat of condensation contrib-

utes proportionately more than ΔH_m and solubility decreases with increasing temperature. Heats of solution of EtO in Teflon-FEP, PVC, and polypropylene are negative (exothermic) and solubility decreases as expected with increasing temperature. Heats of solution in polyethylene, however, are positive (endothermic) despite the fact that EtO is a very condensible vapor; its normal boiling point is 10.5°C.[43] Aboul-Nasr and Huang[44] encountered the same phenomenon when studying the sorption of benzene and hexane in modified polyethylene films, and explained it qualitatively in terms of relative changes in segmental mobility of the polymer chains and changes in condensibility. As temperature increases the vapor becomes increasingly less condensible. However, at the same time the segmental mobility increases which allows more vapor molecules to become sorbed at the interface. Depending on which effect predominates, solubility may increase or decrease with temperature. For ethylene oxide in polyethylene, it appears that the decrease in condensibility of penetrant is offset by the large increase in chain mobility.

Between 20°C and 60°C the average heat of condensation of ethylene oxide is about −5700 cal/mol (38). Hence, Eq. (20) reduces to

$$\Delta H_s = -5700 + \bar{V}_1(\delta_1 - \delta_2)^2 \tag{21}$$

if we assume that $\phi_2 \approx 1$. If the simple two-stage model outlined above is valid, then as the solubility parameters of the polymer and penetrant become more nearly equal the heat of solution becomes, in turn, more exothermic or less endothermic. Table III shows this to be true for four of the six films. Thus, sorption of ethylene oxide in polyethylene and polyvinylchloride can be described, at least qualitatively, by the simple two-stage model and therefore probably follows Henry's law.

A closer examination of Eq. (21) reveals that because the second term is always positive, ΔH_s cannot be greater (more exothermic) than −5700 cal/mol. However, the heat of solution of EtO in Teflon-FEP is approximately −9 kcal/mol, significantly larger than the limiting value prescribed by Eq. (21). When studying the diffusion of isobutane and propane in glassy polycarbonate, Chen[33] also found that the sum of ΔH_c and ΔH_m left roughly −5 kcal/mol of solution enthalpy unaccounted for. He hypothesized that the excess enthalpy could be accounted for by the increased solubility of the permeants in the glassy polymer. The nonequilibrium glass contained excess free volume in the form of microvoids and it was the temperature dependence of this free volume that gave rise to the additional enthalpy. The existence of two modes of sorption (Henry's law sorption and sorption in microvoids) has been described by the dual-mode sorption model.[45] It accounts for the large negative enthalpies of solution in some polymer glasses. The observation here of excess enthalpy in the solubility of EtO in Teflon-FEP bears further investigation to determine the precise nature of the sorption mechanism. If indeed dual sorption occurs, then the solubility coefficients for EtO in Teflon-FEP represent pseudo-Henry's law constants which include contributions from ordinary dissolution and also from microvoid sorption.

CONCLUSIONS

Using a simple apparatus based on the carrier gas method of measurement, estimates of permeability, diffusion, and solubility coefficients describing the transport of ethylene oxide through several polymer films have been obtained. The results indicate that at the partial pressure of EtO to which the films were exposed, diffusion in polyethylene is concentration independent and Fickian. This simple diffusion model is also likely valid for the other films investigated. Two different methods were used to evaluate the diffusion coefficient, and, within the precision of the data, they yield the same results. The observation of excess enthalpy in the solubility of EtO in Teflon-FEP copolymer suggests the possibility of dual-mode sorption, although more work is needed to confirm this.

The authors would like to thank K. Beirnes for measuring the crystalline content and the glass transition temperatures of the films. One of us (A. P.) would like to thank the Natural Sciences and Engineering Research Council of Canada for an NSERC Scholarship during the course of the work.

References

1. *Kirk-Othmer Encyclopedia of Chemical Technology*, Vol. 21, Wiley Interscience, New York, 1983, p. 637.
2. I. Sax, *Dangerous Properties of Industrial Materials*, 4th ed., Van Nostrand Reinhold Ltd., New York, 1975, p. 741.
3. N. I. Komarkova and T. V. Likhtman, *Biomed. Eng.*, **17**(3), 95 (1983).
4. R. Y. M. Huang and P. J. F. Kanitz, *J. Appl. Polym. Sci.*, **13**, 669–683 (1969).
5. P. J. F. Kanitz and R. Y. M. Huang, *J. Appl. Polym. Sci.*, **14**, 2739–2751 (1970).
6. R. Y. M. Huang and P. J. F. Kanitz, *J. Macromolec. Sci. (Physics)*, **B5**(1), 71–88 (1971).
7. P. J. F. Kanitz and R. Y. M. Huang, *J. Appl. Polym. Sci.*, **15**, 67–82 (1971).
8. R. W. MacDonald and R. Y. M. Huang, *J. Appl. Polym. Sci.*, **26**, 2239–2263 (1981).
9. T. L. Caskey, *Mod. Plastics*, **45**, 148 (1967).
10. K. D. Ziegel, H. K. Frensdorff, and D. E. Blair, *J. Polym. Sci.*, **7**, 809 (1969).
11. R. A. Pasternak, J. F. Schimsheimer, and J. Heller, *J. Polym. Sci.*, **8**, 167 (1970).
12. D. G. Pye, H. H. Hoehn, and M. Panar, *J. Appl. Polym. Sci.*, **20**, 287 (1976).
13. H. Yasuda and K. Rosengren, *J. Appl. Polym. Sci.*, **14**, 2839 (1970).
14. T. L. Smith and R. E. Adam, *Polymer*, **22**, 299 (1981).
15. R. M. Felder, R. D. Spence, and J. K. Ferrell, *J. Appl. Polym. Sci.*, **19**, 3193 (1975).
16. L. J. Murray and R. J. Dorschner, *Package Eng.*, **56**, 76 (1983).
17. M. Uchikura, H. Odani, and M. Kurata, *Kobunshi Ronbunshu*, **39**(3), 149 (1982).
18. M. Sipek, V. Jehlicka, and N. Xuan Quang, *Chem. Listy*, **76**(3), 273 (1982).
19. S. P. Chen, *Am. Chem. Soc., Div. Polym. Chem., Polym. Prepr.*, **15**, 77 (1974).
20. M. Chainey, M. C. Wilkinson, and J. Hearn, *J. Appl. Polym. Sci.*, **23**, 2947 (1985).
21. V. Stannett, in *Diffusion in Polymers*, J. Crank and G. S. Park, eds., Academic Press, London, 1968, p. 45.
22. J. Crank, *The Mathematics of Diffusion*, 2nd ed., Oxford University Press, London, 1975, p. 2.
23. H. B. Hopfenberg and H. L. Frisch, *J. Polym. Sci.*, **7**, 405 (1969).
24. M. Lomax, *Polym. Test.*, **1**(2), 105 (1980).
25. M. Lomax, *Polym. Test.*, **1**(3), 211 (1980).
26. R. M. Barrer, *Trans. Faraday Soc.*, **35**, 628 (1939).
27. R. M. Felder and G. S. Huvard, in *Methods of Experimental Physics*, Vol. 16, C, R. A. Fava, ed., Academic Press, New York, 1980, pp. 320–321.
28. S. P. Chen and J. A. D. Edin, *Polym. Eng. Sci.*, **20**(1), 40 (1980).
29. R. M. Felder, C.-C. Ma, and J. K. Ferrell, *A.I.Ch.E. J.*, **22**(4), 724 (1976).
30. T. Duncan, W. J. Koros, and R. M. Felder, *J. Appl. Polym. Sci.*, **28**(1), 209 (1983).

31. J. N. Driscoll, *Am. Lab.*, **9**(10), 71 (1976).

32. R. Waack, N. H. Alex, H. L. Frisch, V. Stannett, and M. Szwarc, *Ind. Eng. Chem.*, **47**, 2524 (1955).

33. S. P. Chen, *Am. Chem Soc., Div. Polym. Chem., Polym. Prepr.*, **24**(1), 95 (1983).

34. A. S. Michaels and R. B. Parker, *J. Polym. Sci.*, **41**, 53 (1959).

35. A. Phatak, M.A.Sc. Thesis, University of Waterloo, Waterloo, Ontario, 1985.

36. A. Rudin, *The Elements of Polymer Science and Engineering*, Academic Press, New York, 1982, p. 436.

37. J. Brandrup and E. Immergut, *Polymer Handbook*, Second Edition, Wiley, New York, 1975, IV-349.

38. N. L. Thomas and A. H. Windle, *Polymer*, **6**(6), 613 (1980).

39. H. B. Hopfenberg and V. Stannett, "The Diffusion and Sorption of Gases and Vapours in Glassy Polymers," in *The Physics of Glassy Polymers*, R. N. Haward, ed., John Wiley and Sons, New York, 1980.

40. J. Brandrup and E. Immergut, in *The Physics of Glassy Polymers*, R. N. Haward, ed., John Wiley and Sons, New York, 1980.

41. G. J. Amerongen, *J. Polym. Sci.*, **5**, 307 (1950).

42. C. E. Rogers, in *Physics and Chemistry of the Organic Solid State*, Vol. 2, D. Fox, M. Labes, and A. Weissberger, eds., Interscience Publishers, New York, 1965, p. 535.

43. R. C. Reid, J. M. Prausnitz, and T. K. Sherwood, *The Properties of Gases and Liquids*, 3rd ed., McGraw-Hill Book Company, New York, 1977, Appendix A.

44. O. T. Aboul-Nasr and R. Y. M. Huang, *J. Appl. Polym. Sci.*, **23**, 1851 (1979).

45. H. B. Hopfenberg and V. Stannett, *J. Appl. Polym. Sci.*, **23**, 508 (1979).

Received September 15, 1986
Accepted December 11, 1986